2.3 Characterization of the Final Precursor Alloy to a Larger Best Practice Heat of 14YWT[1] — N. J. Cunningham, Y. Wu, G. R. Odette. D. Gragg, and K. Fields (University of California Santa Barbara) D. T. Hoelzer (Oak Ridge National Laboratory), S. A. Maloy (Los Alamos National Laboratory)

OBJECTIVES

The objective of this work was to characterize the alloy 14YWT-PM2, which is an extruded and cross-rolled precursor alloy to a large heat of 14YWT being produced using an alternative processing path that incorporates Y during gas atomization process.

SUMMARY

We describe our characterization of a new, extruded and cross-rolled nanostructured ferritic alloy (NFA) designated 14YWT-PM2 (PM2). Atomized Fe14Cr powders containing Y, Ti, and W were milled for 40 h with FeO, extruded at 850°C, and cross-rolled at 1000°C. The consolidated alloy was characterized by transmission electron microscopy (TEM) and atom probe tomography (APT), as well as by various mechanical property tests. A summary of the TEM, APT, mechanical testing results are shown in Table 1. PM2 contains a high number density of $N = 8.4\pm2.6\times10^{23}$ m^{-3}, small <d> = 1.75±0.35 nm Y-Ti-O nanofeatures (NFs). The balance of the microstructure consists of: a) a fine, nearly unimodal size distribution of grains with approximately equiaxed cross sections, that are moderately extended in the extrusion direction, with an average effective diameter $d_g \approx 424$ nm; and, b) a high dislocation density of $r \approx 1.2\times10^{15} m^{-2}$. Larger Ti oxi-nitride precipitate phases are also observed. The corresponding $\mu H = 401\pm15$ kg/mm^2, is consistent with yield and ultimate strengths of 1125 and 1298 MPa, respectively. The cleavage fracture toughness of PM2 increases in the temperature regime from ≈ -200 to -100°C up to a ductile tearing upper shelf transition at ≈ 80 MPa√m. A limited number of strain rate jump creep tests also showed high strength, comparable to that of the strongest NFA, in spite of the formation of edge cracks and possible necking during loading.

In addition, milled powders annealed at 850ºC, 1000ºC and 1150ºC were characterized by small angle neutron scattering (SANS) and TEM. They also contained a high number density of NFs with increasing <d> and decreasing (N) and volume fraction (f) with increasing temperature.

BACKGROUND

Nanostructured ferritic alloys (NFAs) have applications in advanced fission and fusion reactors and are strengthened and made irradiation tolerant by a high number density of thermally stable Y-Ti-O nanofeatures (NFs). The conventional NFA processing path uses ball milling to mechanically alloy Y_2O_3 in the Fe-Cr matrix, which is expensive and often leads to heterogeneous distributions of NFs. To overcome these challenges an alternative processing path in which Y is included in the melt prior to gas atomization and rapid solidification was developed in collaboration with partner institutions including Oak Ridge National Lab, Los Alamos National Lab, ATI Powder Metals, UC Berkeley and South Dakota School of Mines.

[1]This research was primarily sponsored by the DOE Office of Nuclear Energy under NEUP grants and a LLNL subcontract to UCSB. However, the FusMat program is using PM2 for various irradiation studies so it is appropriate to report these results in the a Fusion Semiannual Report.

Many small lab heats of NFA were prepared using this alternative processing method and analyzed in a program primarily funded by the DOE Office of Nuclear Energy [1]. The results of this extensive effort were used to identify the best processing practices. This preliminary work culminated in the final production of an extruded and hot, cross-rolled heat at ORNL known as 14YWT-PM2 (PM2). The following report describes the characterization of this new material.

STATUS AND PROGRESS

ATI Powder Metals (Pittsburgh, PA) produced the 14YWT atomized powders in its Laboratory Gas Atomizer (LGA) with a 27 kg (nominal) capacity vacuum induction melting (VIM) furnace lined with an alumina crucible. The crucible tilts to pour the melted alloy into a refractory tundish with a ceramic nozzle at the bottom. The combined effects of gravity and aspiration pressure deliver the melt through the nozzle to the gas atomization die in a close-coupled mode consisting of coaxial, co-directional supersonic gas flow to disrupt the stream of molten metal. Atomization breaks the melt stream into spheroidal droplets that solidify rapidly in an Ar or He atmospheres while moving through a stainless steel cooling tower. The objective is to solute trap Y in solution. Unfortunately this did not occur and the powder cellular solidification microstructure contained phase separated Y, mostly in ≈100 nm $Fe_{17}Y_2$ boundary precipitates or Y-rich precipitates within the grains. In addition, the large batch of powders prepared for subsequent industrial milling in greater quantities by Zoz Corporation in Germany, had a low O content, which was previously found to be inadequate to form fine dispersions of Y-Ti-O NFs [2]. Therefore, attritor ball milling was required both to adequately mix the Y and to add O. The PM2 powder was Zoz CM08 attritor milled at ORNL for 40 h with FeO (-10 mesh, Alpha Aesar, Part #30513) to increase the O content to ≈ 0.135 wt.%. The milling used 5 mm hardened steel balls at a ball to powder mass ratio of 10:1. The milling speed alternated between 900 (2 minutes) and 450 rpm (9 minutes). Care was used to limit O and N contamination from the atmosphere by better chamber sealing and evacuating and backfilling with Ar several times. The powders were then canned and degassed at 400ºC, hot extruded at 850º, annealed for 1 h at 1000ºC and hot cross-rolled to a ≈ 50% thickness of 5 mm. Optical microscopy, SANS, APT and TEM was performed on the extruded and cross-rolled alloy. The volume of available consolidated PM2 was approximately 14 cm^3, allowing for limited mechanical property measurements, including μH, tensile, strain rate jump creep and fracture testing.

Table 1. Summary of the PM2 characterization results.

NFs	
TEM <d> (nm) APT <d> (nm)	1.4 2.1
Average <d> (nm)	1.75±0.35
TEM N (10^{23} m^{-3}) APT N (10^{23} m^{-3})	5.8 11.0
Average N (10^{23} m^{-3})	8.4±2.6
TEM f (%) APT f (%)	0.07 0.47
Average f (%)	0.27±0.2
EDX Y/Ti	0.5 -1
APT Y/Ti/O	12/43/45
Other Microstructures	
Dislocation density (m^{-2})	$1.2x10^{15}m^{-2}$
Average grain size	424 nm
Mechanical Properties	
μH (kg/mm^2)	401±15
Yield Stress, LX(MPa)	1125
Ultimate tensile stress, LX (MPa)	1298
Elongation to a load drop (%)	6
Total Elongation	11
Temperature ≈ half way between lower and upper shelf toughness (°C)	-170
LMP estimation of the stress at 750°C, for a 10^{-8}/s creep rate - axial/transverse (MPa)	310/260

Limited SANS and TEM studies were performed on milled powders annealed at 850, 1000 and 1150ºC for 3 h. The baseline anneals involved a 15ºC/min ramp to temperature and cooling, but one condition was an isotherm anneal at 1150ºC.

Microstructural Characterization

The TEM micrographs in Figures 1a and b show a moderately elongated grain structure in the extrusion direction, with an effective grain diameter of 424 nm. The SEM back-scattered images in Figures 1c and d show a more isotropic grain structure in the plane normal to the extrusion direction. At these high magnifications PM2 appears to have a uni-modal grain size distribution in the areas probed. In contrast, previous work on alloys consolidated at 1150ºC showed a bimodal grain size distributions with the smallest grains a few hundred nm in diameter and a significant fraction of larger grains up to 10 μm in diameter.

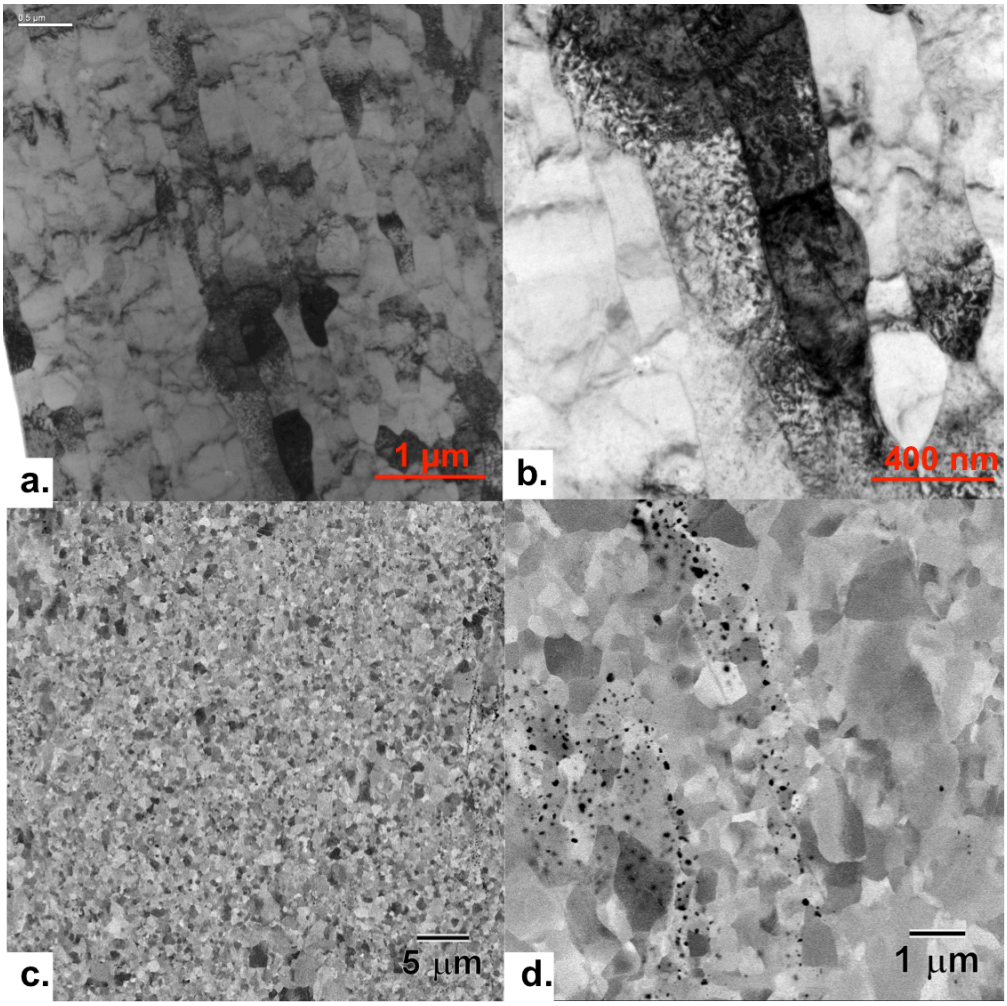

Figure 1. a-b) TEM micrographs perpendicular to extrusion direction showing elongated grain structure; c-d) SEM back-scattered imaging showing fine grain size; the black regions in these micrograph are Ti oxi-nitride phases.

Optical micrographs for chemically etched samples in Figure 2 show the grain structure at lower magnification in three directions. Note that the samples are difficult to etch due to the high Cr content and small grain size. Nevertheless, there appears to be a bimodal grain size distribution perpendicular to the extrusion and rolling direction as shown in Figure 2a. However, the large grain area fraction is small.

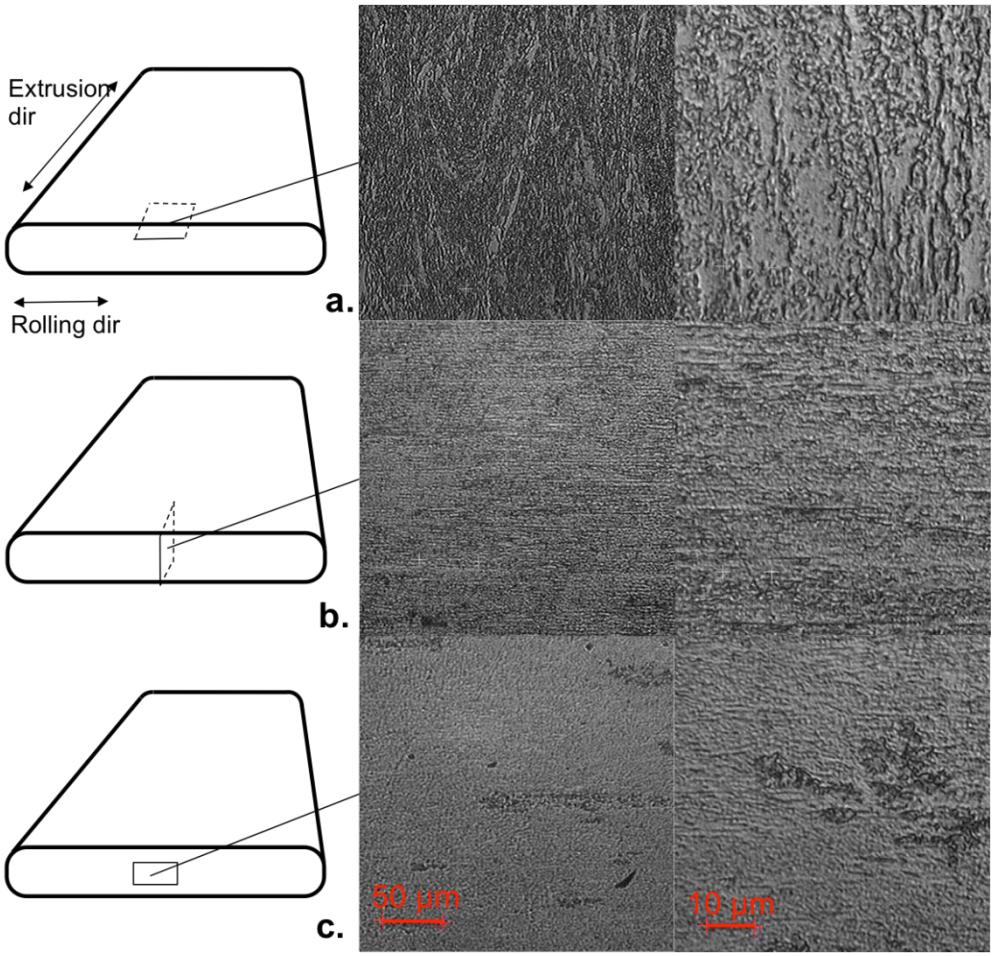

Figure 2. Etched PM2 alloy of surface a) perpendicular to the rolling direction; b) perpendicular to the extrusion direction; c) parallel to the extrusion direction.

TEM also revealed a high density of dislocations. Figure 3 shows two-beam bright field image showing a dislocation density of 1.2×10^{15} m^2.

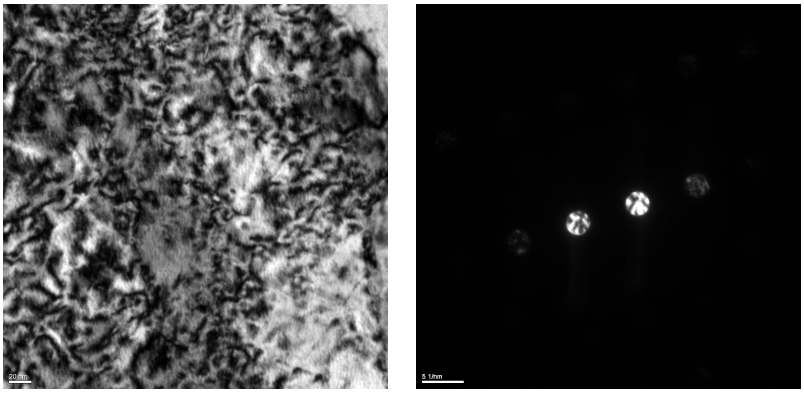

Figure 3. Two-beam bright field TEM image showing high density of dislocations.

The main focus of this research was on characterizing the Y-Ti-O NFs. TEM was first performed on the powder annealed at 1150ºC. Figure 4 shows a high N ≈ $2.1 \times 10^{23}/m^3$ of <d> ≈ 2.8 nm NFs, with a volume fraction f ≈ 0.24. EDX showed a Y/Ti ratio of 0.74 for the NF.

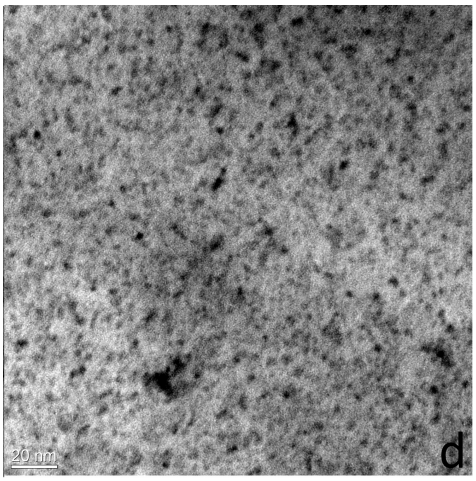

Figure 4. TEM on powder milled with FeO and annealed for 3 h at 1150ºC.

SANS was also performed on four powders milled with FeO for 40 h and annealed for 3 h at 850ºC, 1000ºC, and 1150ºC. Three powders were ramped up to the hold temperature at

5ºC/min and cooled at the same rate to mimic the HIPing time-temperature history. A fourth powder was isothermally annealed at 1150ºC, which is closer to that experienced during extrusion; note the temperature was lower for PM2. Table 2 summarizes the SANS results. The <d> increased and the N and f decreased with increasing annealing temperature. The M/N ratio remained relatively constant. No significant difference was observed between the ramp anneal and isothermal anneal at 1150ºC. SANS has not yet been performed on the consolidated alloy.

Table 2. Summary of the SANS results on milled and annealed powders.

T(°C)-cycle	<d> (nm)	M/N	N ($10^{23}/m^3$)	f (%)
1150 - ramp	2.80	1.2	7.1	0.8
1000 - ramp	2.46	1.1	12.5	1.0
850 - ramp	2.14	1.1	23.4	1.2
1150 - isothermal	2.82	1.2	7.2	0.9

The consolidated PM2 alloy was also analyzed using TEM and APT. TEM measured <d> ≈ 1.4 nm and N ≈ 5.2×10^{23}, indicating smaller and more numerous NF than in the annealed powders. This gives a volume fraction of 0.07%, which is lower than expected and measured by APT. In foil EDX showed the NF to typically have an estimated Y/Ti ratio less than 1. Figure 5 shows a fairly uniform distribution and high number density of NF. Some larger precipitates were found to contain high levels of Ti and N.

An APT atom map with 2% Y-Ti-O iso-concentration surfaces, shown in Figure 6, has uniformly distributed NFs. Only one APT volume of PM2 was analyzed, with N ≈ $11.0 \times 10^{23}/m^3$ and <d> ≈ 2.1 nm. The size distributions of a previous 1150ºC HIP consolidated alloy, OW2, and PM2 are compared in Figure 7.

The bulk, matrix and NF compositions are shown in Table 3. The high nominal Fe content is believed to be an APT artifact due to trajectory aberrations that artificially place matrix inside the NF. The Y/Ti/O ratio is 12/43/45 giving a Y/Ti ratio of 0.29. The Y/Ti ratio in PM2 is similar to alloy MA957. In addition to Y, Ti, and O, PM2 also appears to contain a high Cr content in the NFs. The 1-D profiles in Figure 8a show a reduction in Fe but a slight increase in Cr through the NFs. The 1-D profiles of Y, Ti, and O in both the z and x-y directions show a Ti and O tail below the Y core with more symmetric concentration profiles in the x-y direction. The extra matrix atoms in the NF are known to be artifacts since the atom density in the precipitates increases to non-physical levels as shown in Figure 8b. This increase in density is caused by dimpling of the atom probe tip surface during evaporation when the NF atoms evaporate at lower electric fields than the matrix or when higher electric fields are induced above the NF [3]. The dimpling alters the electric field lines so that matrix atoms at the NF interface are projected inward and thus observed as part of the NF after data reconstruction.

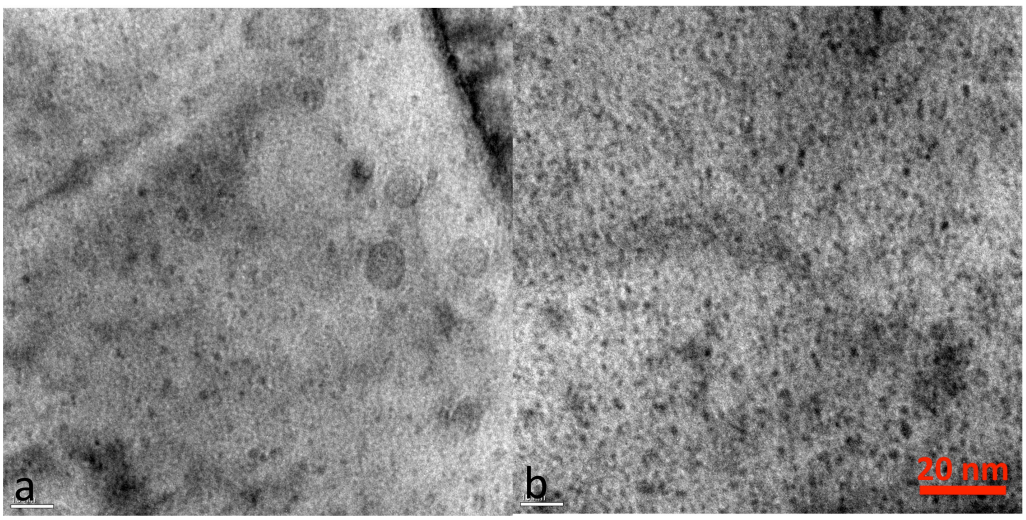

Figure 5. Bright field TEM images of extruded and cross-rolled PM2 alloy.

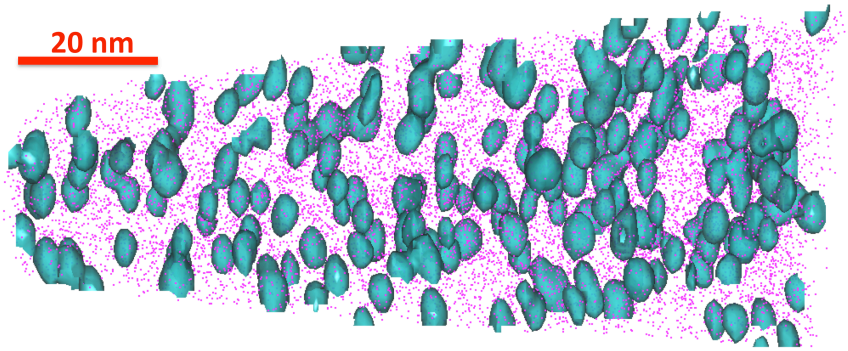

Figure 6. An APT reconstruction of a volume of PM2 analyzed by APT. The NFs are shown by Y-Ti-O iso-concentration surfaces (2.0 at.%).

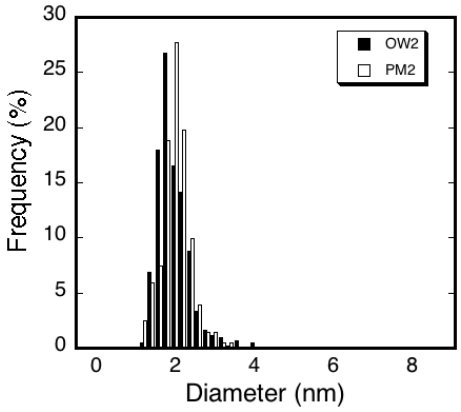

Figure 7. Comparison of the size distribution of NFs in OW2 and PM2.

Table 3. The average APT NF composition (at.%) in PM2.

	Fe	Cr	W	Ti	Y	O	C	Al	Si
Bulk	83.6	14.5	0.952	0.257	0.073	0.342	0.120	0.016	0.075
Matrix	84.2	14.4	0.961	0.059	0.016	0.134	0.108	0.009	0.073
Cluster	72.6	17.3	0.963	3.64	1.05	3.88	0.330	0.132	0.108
Y-Ti-O				42.5	12.3	45.3			

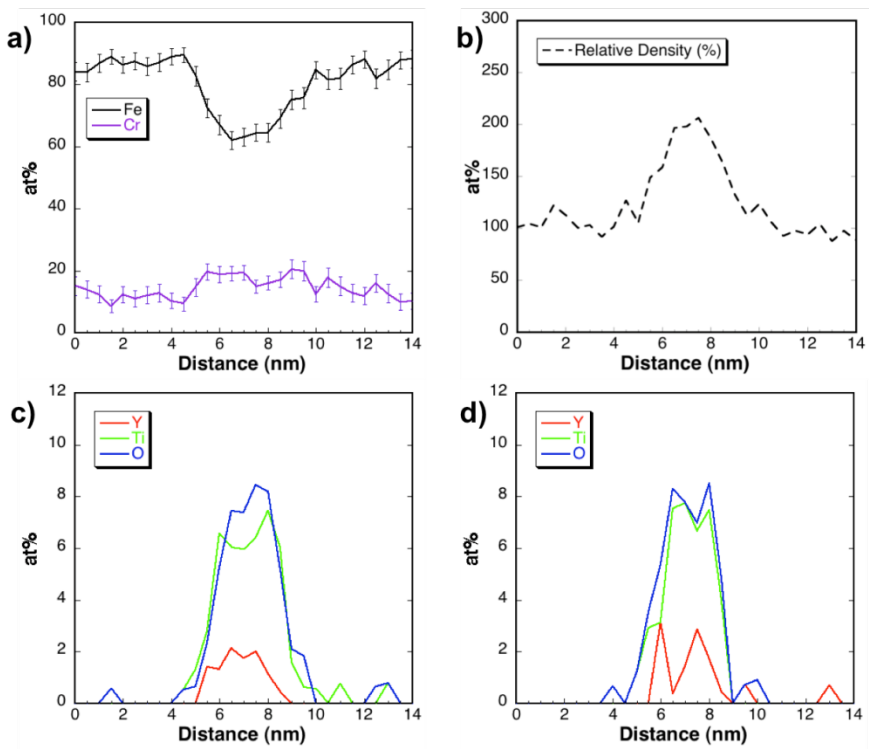

Figure 8. 1-D composition profiles of single NF in PM2 alloy showing a) Fe and Cr content and b) atom density relative to the matrix density in Z direction; c) Z and d) X-Y direction atomic Y, Ti, and O content.

Mechanical Testing

Due to time and material constraints only a limited number of scoping mechanical property tests could be performed. So the results reported here should be generally considered provisional. A hardness of ≈ 401±15 kg/mm^2 was measured on the PM2 surface perpendicular to the extrusion direction. Tensile and creep tests used SSJ2 tensile specimens (4×16×0.5mm) while fracture tests used small bend bars (3.33x3.33x18mm). The tensile and bend bar specimens were oriented as shown in Figure 9. Since there are two deformation orientations we use a modified nomenclature for the bend specimens where the crack propagation path and tensile axis are parallel to the extrusion (LE) or the cross-rolling (LX) directions, while the crack plane normal is transverse to these processing deformation directions.

A yield stress of 1125 MPa and ultimate tensile stress of 1298 MPa was observed in the LX orientation. Thus the ratio of the average of these two stresses with the microhardness value is almost exactly 3. The engineering flow stress has a near plateau between ≈ 1 and 6% strain, indicating limited strain hardening and significant pre-necking uniform elongation. The total elongation was ≈ 11%. An SEM micrograph of the tensile specimen's fracture surface is shown in Figure 10. The material has what appear to be delamination cracks on planes defined by the extrusion and rolling directions. Slightly lower strength was observed in the LE orientation with a yield stress of 1035 MPa and ultimate tensile stress of 1164 MPa, as summarized in Table 4.

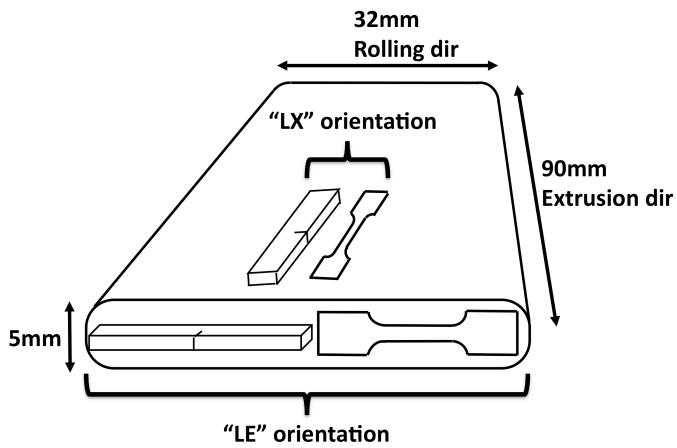

Figure 9. SSJ2 tensile and 1/3 bend bars produced from PM2 extruded and cross-rolled material (not to scale).

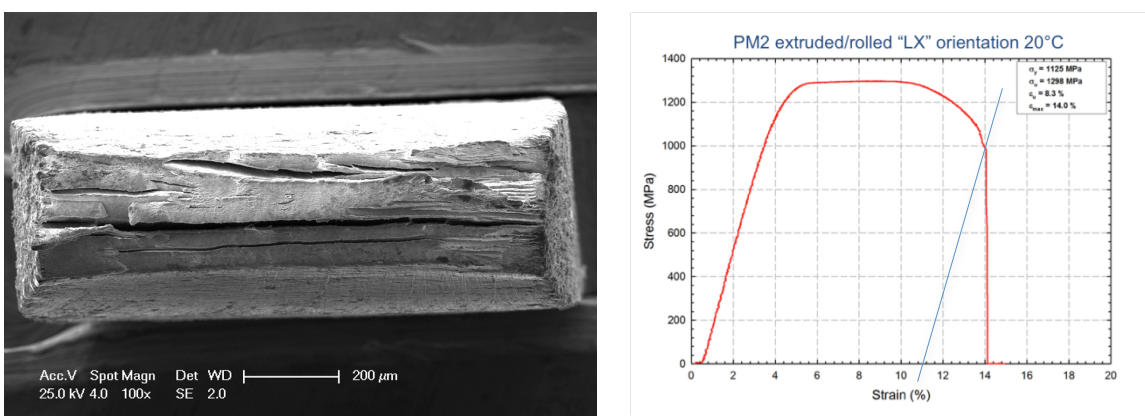

Figure 10. Tensile test fracture surface of PM2 (LX orientation) showing cracks along extrusion and rolling direction.

Table 4. Tensile test results.

T(°C)-cycle	LX	LE
σ_y (MPa)	1125	1035
σ_u (MPa)	1298	1165

Four strain rate jump tests were performed; one in the LE orientation and three in the LX orientation. Stress increases were observed upon application of higher strain rates as expected. However, the stresses did not plateau, but rather slowly decreased with increasing strain. This is believed to be due to development of edge cracks that reduce the load bearing cross section, and possible onset of necking. Thus nominal stresses after the jumps are likely to be less than the actual values, but the results still provide a reasonable basis to estimate the comparative strength of PM2. Future testing will use larger, polished cylindrical specimens, but due to the limited material availability this was not possible for PM2. The strain rates are shown in the Larson-Miller type plot in Figure 12 as filled circles for both orientations. In spite of the fact that these are probably less than the actual stresses, the PM2 strength is higher than either the US and French heats of MA957 and close to that for the Japanese 12YWT that is considered to be one of the strongest NFA variants produced to date.

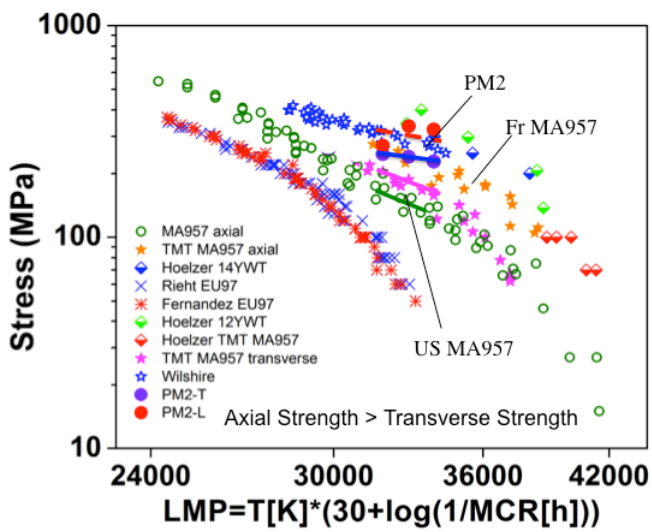

Figure 11. Larson-Miller plot comparing PM2 with other NFA alloys.

Three-point bend bar tests measure fracture toughness of PM2 from -200ºC up to 150ºC for PM2. The results are shown in Figure 12a along with this NFA HIP consolidated at 1150°C and designated OW4. In the latter case the cleavage transition to the upper shelf occurs between 0 and 150°C at ≈ 70 MPa√m (and even lower at 600°C). The high transition temperature is attributed to the large grains and bimodal grain size distribution in this NFA. In contrast the cleavage transition for both orientations of PM2 is much lower, between -200 and -100°C. However, the upper shelf ductile tearing toughness is still low in PM2 at ≈ 80 MPa√m. The

temperature at the mid-point between lower and upper shelf, assumed to be at ≈ 20 and 80 MPa√m, respectively, is ≈ -160°C. The much lower transition temperature in PM2 is attributed to its more uniformly fine grain structure. The low ductile tearing toughness is thought to be due to a high density of coarser scale Ti-oxides or oxi-nitrides that act as microvoid nucleation sites as illustrated to the micrograph in Figure 12b. Figure 12c shows the same type of delamination cracks that are also observed in the tensile test.

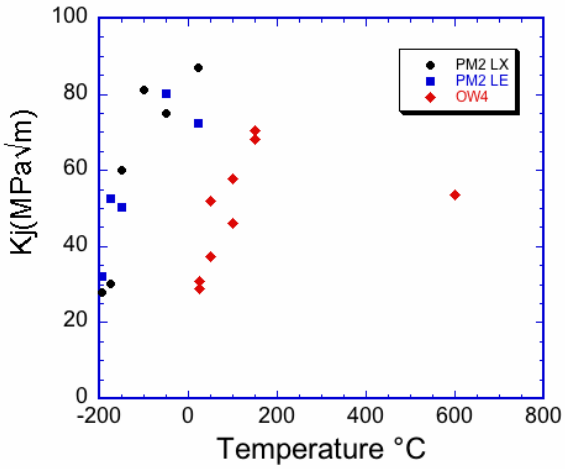

a.

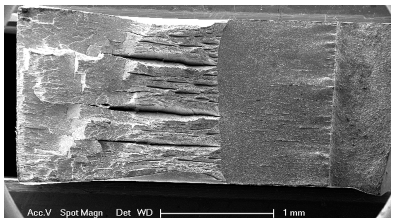

b.

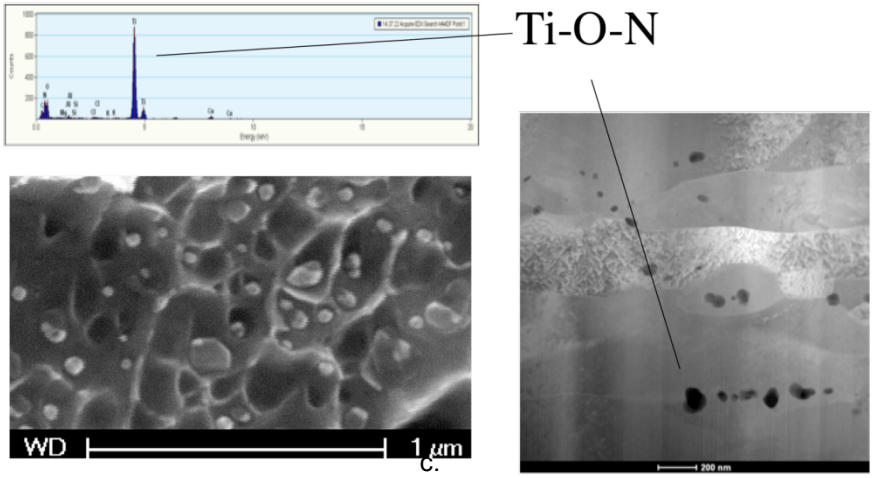

c.

Figure 12. DBTT of OW4 and PM2 in LE and LX orientations; and b) high magnification fracture surface and TEM image showing large Ti-oxi-nitrides; c) low magnification fracture surface of PM2 LX bend bar showing delamination.

FUTURE WORK

SANS will be carried out to complete the characterization of the NF in PM2.

REFERENCES

1. N. J. Cunningham, "Study of the Structure, Composition, and Stability of Y-Ti-O nm-Scale Features in Nano-Structured Ferritic Alloys," Ph.D. Thesis, University of California - Santa Barbara, Santa Barbara, CA (2012).
2. Y. Wu, N. J. Cunningham, A. Etienne, E. Haney, G. R. Odette, "The Effect of Bulk Oxygen Concentration on the Micro-Nanostructure and Strength of a 14Cr Nanostructured Ferritic Alloy," DOE Fusion Reactor Materials Program Semiannual Progress Report for the Period Ending June 30, 2011, DOE/ER-0313/50 2011.
3. C. Oberdorfer and G. Schmitz, "On the Field Evaporation Behavior of Dielectric Materials in Three-Dimensional Atom Probe: A Numeric Simulation," *Microsc. Microanal.* **17**, 2011, 15-25.